Apparently regular octahedral coordination of Ag(II) in IF6[Ag(SbF6)3]

Zoran Mazej, Evgeny Goreshnik, Iztok Arčon, Nataša Zabukovec Logar, Venčeslav Kaučič

Zeitschrift für Anorganische und Allgemeine Chemie

Apparently regular octahedral coordination of Ag(II) in IF6[Ag(SbF6)3]

Journal:	*Zeitschrift für Anorganische und Allgemeine Chemie*
Manuscript ID:	zaac.200900238
Wiley - Manuscript type:	Article
Date Submitted by the Author:	23-Apr-2009
Complete List of Authors:	Mazej, Zoran; Jozef Stefan Institute, Dep. of Inorg. Chem. and Technology Goreshnik, Evgeny; Jozef Stefan Institute Arčon, Iztok; University of Nova Gorica Zabukovec Logar, Nataša; National Institute of Chemistry Kaučič, Venčeslav; National Institute of Chemistry
Keywords:	silver, fluorides, iodine, crystal structure, vibrational spectroscopy

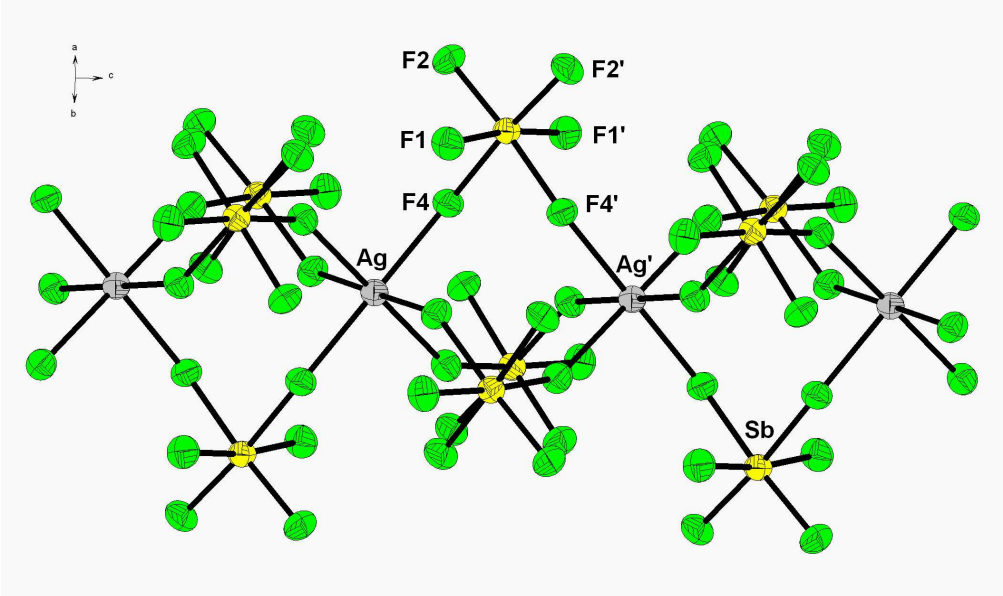

178x106mm (300 x 300 DPI)

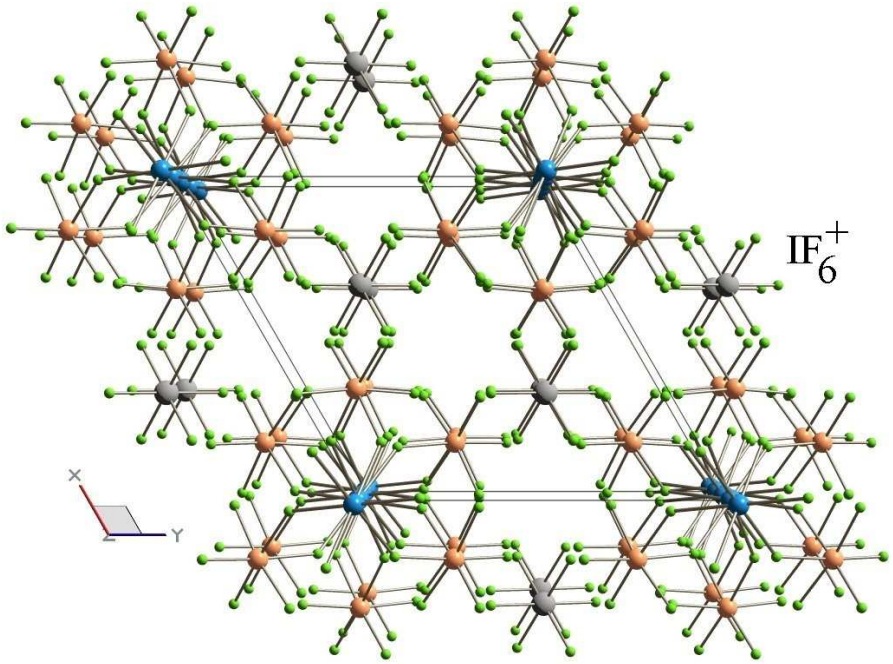
IF_6^+
X
Y

Apparently regular octahedral coordination of Ag(II) in $IF_6[Ag(SbF_6)_3]$

Zoran Mazej,[1] Evgeny Goreshnik,[1] Iztok Arčon,[1,2] Nataša Zabukovec Logar,[3] Venčeslav Kaučič[3]

[1]Jožef Stefan Institute, Jamova 39, SI-1000 Ljubljana, Slovenia

[2]University of Nova Gorica, Vipavska 13, SI–5000 Nova Gorica, Slovenia

[3]National Institute of Chemistry, Hajdrihova 19, Ljubljana, Slovenia

Abstract

Crystal structure of $IF_6[Ag(SbF_6)_3]$ has been determined by X-ray single crystal and X-ray powder diffraction analysis. $IF_6[Ag(SbF_6)_3]$ crystallizes in the trigonal system, space group $P\bar{3}1c$ (No. 163), with a = 10.2676(8) Å, c = 9.5552(10) Å, V = 872.38(13) Å^3 and Z = 2. The structure consists from $[Ag(SbF_6)_3]^-$ chains and $[IF_6]^+$ cations placed between them. Ag^{2+} is found in regular octahedral coordination of six fluorine atoms (Ag–F = 6 x 2.170(12) Å). EXAFS analysis of Jahn-Teller distortions in $IF_6[Ag(SbF_6)_3]$ shows that Ag^{2+} surrounding is elongated octahedral at room temperature. EXAFS signals are fitted with four short and two long Ag–F distances (4 x 2.11(1) Å; 2 x 2.40(2) Å). This result is in apparent contradiction with X-ray diffraction studies where $[AgF_6]$ moiety appears to be regular octahedra.

Raman spectrum of $IF_6[Ag(SbF_6)_3]$ is in agreement with the presence of regular IF_6 and deformed SbF_6 groups.

Introduction

Compounds of Cu^{2+} with its d^9 electron configuration are strongly affected by the Jahn–Teller effect. Cu^{2+} cations are usually found in an elongated octahedral geometry. Orientational disorder of so distorted octahedra can result in too high crystallographic space group symmetry and Cu^{2+} cations in an apparently regular coordination geometry.[1,2] According to the literature data no such case is known for Ag^{2+} which also has d^9 electronic configuration. In all known compounds, where Ag^{2+} is six-fold co-

ordinated, AgL_6 (L = ligand) octahedra are elongated or compressed.[3] The second reason for the apparently regular octahedral coordination of Ag(II) in $IF_6[Ag(SbF_6)_3]$ could be the trifold twinning of the monoclinic or orthorhombic unit cell, resulting in a pseudo trigonal/hexagonal lattice.[4,5] In this work we describe first such case where according to crystallographic data Ag^{2+} is found in an apparently regular octahedral coordination, meanwhile EXAFS analysis shows the presence of tetragonally elongated AgF_6 octahedra.

2. Experimental

2.1. Apparatus and Reagents

Volatile materials (anhydrous HF, F_2) were handled in an all PTFE vacuum line equipped with PTFE valves. The manipulation of the non-volatile materials was done in a dry box (M. Braun). The residual water in the atmosphere within the dry-box never exceeded 2 ppm. The reactions were carried out in FEP (tetrafluoroethylene-hexafluoropropylene) reaction vessels (height 250–300 mm with inner diameter 15.5 mm and outer diameter 18.75 mm) equipped with PTFE valves and PTFE coated stirring bars. Prior to their use all reaction vessels were passivated with elemental fluorine.

IF_6SbF_6 was prepared by reaction between IF_7 and SbF_5 in anhydrous hydrogen fluoride (aHF). IF_7 has been synthesized by fluorination of KI at 250 ^oC. $Ag(SbF_6)_2$ was prepared from AgF_2 and SbF_5/HF mixture as described previously.[6] AgF_2 was obtained by fluorination of $AgNO_3$ in aHF, meanwhile SbF_5/HF mixture was prepared by fluorination of SbF_3 in aHF. Anhydrous HF (Fluka, Purum) was treated with K_2NiF_6 (Ozark Mahoning) for several hours prior to use.

2.2. Raman Spectroscopy

Raman spectra with, a resolution of 2 cm^{-1}, were recorded (10–20 scans) on a Renishaw Raman Imaging Microscope System 1000, with the 632.8 nm exciting line of a He-Ne laser (50 mW).

2.3. X–ray powder diffraction analysis

X-ray powder diffraction pattern was collected at room temperature on a PANalytical X'Pert PRO diffractometer using CuKα radiation (1.54178 Å). The sample was loaded into quartz capillary (0.3 mm) in a dry-box in order to avoid hydration of the sample. The XRPD data were collected in the 2θ range from 10 to 80º 2Θ in steps of 0.033º 2Θ with a total measurement time of 16 hours. The qualitative and quantitative powder analysis of the collected XRPD pattern was performed using the Crystallographic Search-Match programs [7] and TOPAS V2.1 Rietveld refinement program [8].

2.4. EXAFS analysis

The Ag *K*-edge EXAFS data of the $IF_6[Ag(SbF_6)_3]$ sample were obtained in a standard transmission mode at the C station of HASYLAB synchrotron facility, DESY (Hamburg, Germany). A Si(311) double-crystal monochromator was used with 3 eV resolution at 25514 eV. Harmonics were effectively eliminated by detuning the monochromator crystal using a stabilization feedback control. The three ionisation cells were filled with Kr, the first at the pressure of 180 mbar, the second and third at the pressure of 1000 mbar Kr.

The absorption spectra were measured within the interval [from –250 eV to 1000 eV] relative to the Ag *K*-edge. In the XANES region equidistant energy steps of 0.5 eV were used, while for the EXAFS region equidistant *k*-steps ($\Delta k \approx 0.03$ Å^{-1}) were adopted with an integration time of 2s/step. Three repetitions were superimposed to improve signal-to-noise ratio. In all experiments the exact energy calibration was established with simultaneous absorption measurements on 25 μm thick Ag metal foils placed between the second and the third ionization chamber.

The compound in the form of fine powder was pressed into self-supported homogeneous pellet (140 mg/cm^2) in a dry-box to prevent hydrolysis and sealed in inert atmosphere into thin-walled FEP tube. The absorption thickness of the pellet was about 1.5 above the Ag K-edge absorption edge. The FEP tube containing the pellet was mounted on a sample holder in a vacuum chamber of the beam-line. The sealed sample was perfectly stable for several hours of the experiment: no sign of hydrolysis was observed after demounting. The stability of the sample was also confirmed by the reproducibility of the consecutive scans.

2.5. Synthesis of $IF_6[Ag(SbF_6)_3]$

IF_6SbF_6 0.480g (1.0 mmol) and $Ag(SbF_6)_2$ 580 mg (1.0 mmol) were loaded in a reaction vessel in a glove-box. aHF (6 mL) and ~ 5 mmol F_2 were condensed onto the reaction mixture and the reaction vessel was brought to room temperature. The elemental fluorine was added to prevent possible reduction of Ag^{2+} and I^{7+} due to the possible presence of traces of hydrogen or other impurities in aHF. The reaction vessel was warmed to ambient temperature. Beside blue-sky solution, insoluble solid of the same color was observed. After 24 h of intense stirring, the volatiles were pumped off at ambient for four hours, leaving blue-sky colored solid (final mass of $IF_6[Ag(SbF_6)_3]$: 1.040 g). Raman spectrum was recorded, X-ray powder diffraction pattern was taken and EXAFS analysis was done. On the exposure to air $IF_6[Ag(SbF_6)_3]$ immediately decomposes and turns brown.

2.6. Crystal Growth of $IF_6[Ag(SbF_6)_3]$

Single crystals growth was carried out in a double T−shaped apparatus consisting of two FEP tubes (19 mm. o.d., and 6 mm. o.d.). $IF_6[Ag(SbF_6)_3]$ (approximately 150 mg) was loaded into the wider arm of the crystallization vessel in a dry-box. aHF (~3 mL) was then condensed onto the starting material at 77 K. The crystallization mixture was brought up to ambient temperature and the clear blue-sky solution, which had developed, was decanted into the narrower arm. The evaporation of the solvent from this solution was carried out by maintaining a temperature gradient corresponding to about 10 K between both tubes for 5 weeks. The effect of this treatment was to enable aHF to be slowly evaporated from narrower into wider tube leaving the crystals. Selected single crystals of $IF_6[Ag(SbF_6)_3]$ were placed inside 0.3 mm quartz capillaries in a dry-box and their Raman spectra recorded.

2.7. X-ray single crystal structure determination

Crystals were immersed in perfluorinated oil (ABCR, FO5960) in the dry box, selected under a microscope, and transferred into the cold nitrogen stream of the diffractometer. Data were collected on Rigaku AFC7S diffractometer equipped by

Mercury CCD area detector using graphite monochromated MoK_α radiation. The data were corrected for Lorentz and polarization effects, and multi-scan absorption correction was applied. The structure was solved by direct methods using SIR-92 [9] program implemented in program package TeXsan [10] and refined with SHELXL-97 [11] software (program packages TeXsan and WinGX [12]). Structure drawings were generated by Diamond 3.1 software [13], and Balls & Sticks, freely available software [14]. The crystal data and the details of the structure refinement are given in Table 1, selected distances and bond lengths in Table 2.

X-ray crystallographic files in CIF format have been sent to Fachinformationzentrum Karlsruhe, abt. PROKA, 76344 Eggenstein-Leopoldshafen, Germany as supplementary material No. SUP CSD–420464, and can be obtained by contacting FIZ (quoting the article details and corresponding SUP number).

3. Results

3.1. X-ray single crystal structure determination data

The crystal data and the details of structure refinement are given in Table 1.

Table 1. Summary of Crystal Data and Refinement Results for $IF_6[Ag(SbF_6)_3]$

Chemical formula	$IF_6[Ag(SbF_6)_3]$
mol wt (g mol^{-1})	1056.02
Crystal system	trigonal
space group	$P\bar{3}\,1c$
a (Å)	10.2676(8)
c (Å)	9.5552(10)
V (Å^3)	872.38(13)
T (K)	200
Z	2
ρ_{calcd} (g cm^{-3})	4.02
μ (mm^{-1})	7.7
R_1[a]	0.0633
wR_2[b]	0.1608
GOF[c]	1.174

[a] $R_1 = \Sigma||F_o| - |F_c||/\Sigma|F_o|$. [b] $wR_2 = [\Sigma w(F_o^2 - F_c^2)^2/\Sigma(w(F_o^2)^2]^{1/2}$. [c] GOF = $[\Sigma w(F_o^2 - F_c^2)^2/(N_o - N_p)]^{1/2}$, where N_o = no. of reflns and N_p = no. of refined parameters.

In the crystal structure of $IF_6[Ag(SbF_6)_3]$ the neighboring silver atoms are linked via three $[SbF_6]^-$ units, with bridging fluorine atoms in *cis* positions, into infinite –Ag–(*cis*-η^2-$SbF_6)_3$–Ag– chains that are parallel to the *c*–axis (Figure 1). IF_6^+ cations are placed between the chains and interconnected with them with electrostatic interactions forming a tri-dimensional network (Figure 2). Selected bond distances and angles are summarized in Table 2.

Figure 1. Part of the crystal structure of $IF_6[Ag(SbF_6)_3]$ showing infinite –$[Ag(SbF_6)_3]$– chains running along *c*-axis. (ORTEP)

Figure 2. Packing of the –Ag–(*cis*-η^2-$SbF_6)_3$–Ag– chains and IF_6^+ cations in the crystal structure of $IF_6[Ag(SbF_6)_3]$.

Table 2. Selected Bond Lengths (Å) and Bond Angles (°) in $IF_6[Ag(SbF_6)_3]$

Ag–F4	6 x 2.189(7)	I–F3	6 x 1.778(7)
Sb–F2	2 x 1.839(7)	Ag–F4–Sb	140.9(4)
Sb–F1	2 x 1.848(7)		
Sb–F4	2 x 1.933(7)		

3.2. X-ray powder diffraction analysis

The X-ray powder diffraction analysis confirmed the structure solution obtained by the single-crystal structure analysis. The examination of phase purity revealed the presence some additional low-intensity diffraction peaks, that did not belong the $IF_6[Ag(SbF_6)_3]$ phase. The maximum at 23.3 ° 2θ with the relative intensity of 4% and some other peaks with relative intensities less than 1% could be attributed to the $IF_4Sb_2F_{11}$ phase.[15] However, due to the overlapping of the peaks of both phases the presence of $IF_4Sb_2F_{11}$ or some other phases could not be reliably confirmed, but does not exceed a few percents.

In the final Rietveld refinement only main phase $IF_6[Ag(SbF_6)_3]$ has been taken into account. The diffraction peaks profiles were approximated using Double-Voigt approach. The refined parameters were zero shift, scale factor, 8 background polynomial parameters, 5 profile parameters for microstrain and crystallite size, 4 parameters for preferential orientation and lattice parameters. The refinement revealed an acceptable agreement between calculated and observed powder patterns with R_{wp} 1.97% (Supplementary material).

3.3. EXAFS analysis

The quantitative analysis of EXAFS spectra was performed with the IFEFFIT program packages [16]. Structural parameters were quantitatively resolved by comparing the measured signal with model signal, constructed ab initio with the FEFF6 program code [17] in which the photoelectron scattering paths were calculated ab initio from the presumed distribution of neighboring atoms around Ag, based on the proposed XRD crystal structure of $IF_6[Ag(SbF_6)_3]$, which predicts that Ag atom is octahedral coordinated

to six fluorine atoms at 2.19 Å in the nearest coordination shell, followed by consecutive shells of six F at 3.61 Å , six Sb at 3.89 Å, six F at 3.92 Å, six F at 4.53 Å, six F at 4.73 Å and two Ag atoms at 4.78 Å.

The EXAFS model comprised all nearest Ag coordination shells around the central Ag atom, including all single scattering paths and all significant multiple scattering paths up to 4.8 Å. For the first coordination shell with six nearest fluorine atoms, the Jahn-Teller distorted octahedral geometry was taken into account, with four short and two long Ag–F bonds. Similar split was introduced also for the fourth coordination shell composed of F atoms originating from the octahedron around nearest Ag neighbor.

The k^3-weighted Ag EXAFS spectrum of the $IF_6[Ag(SbF_6)_3]$ sample and its Fourier-transform is shown in Figures 3 and 4, together with a best-fit EXAFS model.

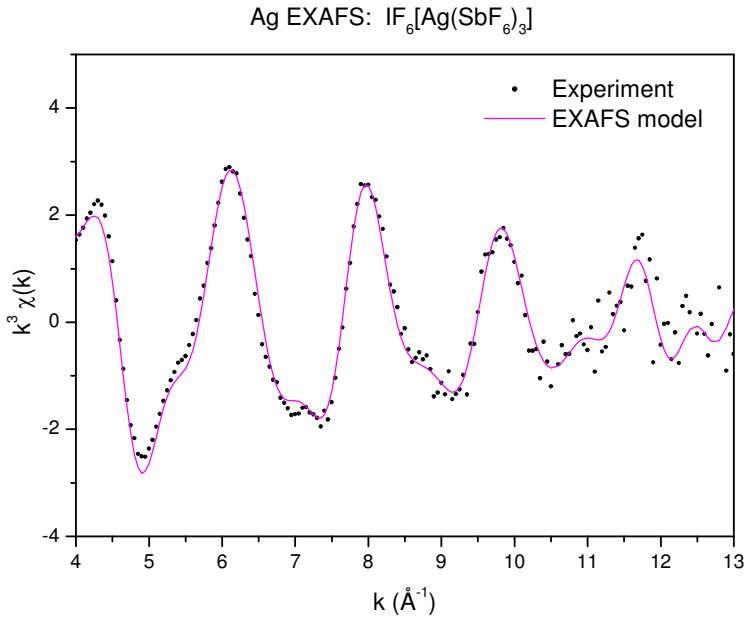

Figure 3. The k^3-weighted Ag EXAFS spectrum of the $IF_6[Ag(SbF_6)_3]$ sample, Experiment – (dots); EXAFS model – (solid line).

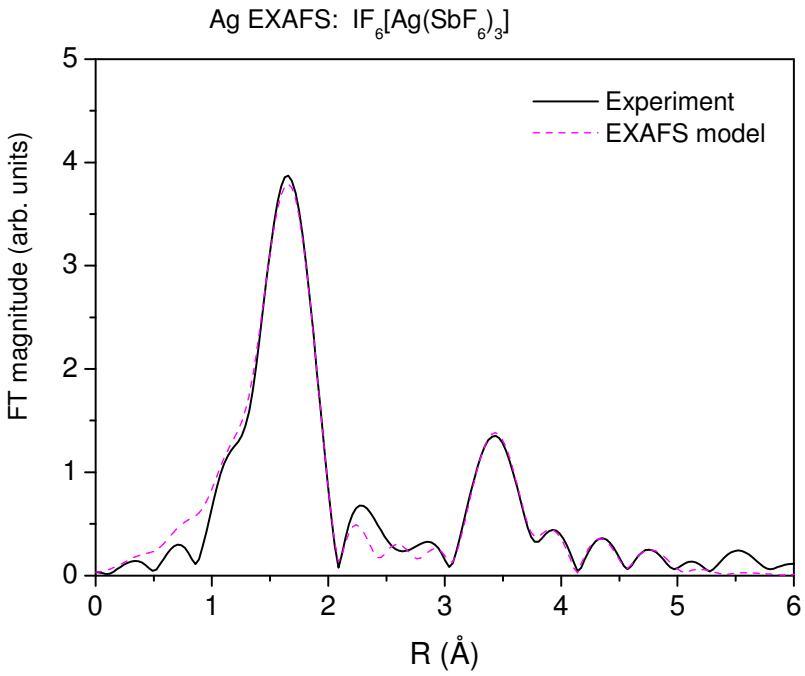

Figure 4. Fourier transform of k^3-weighted Ag EXAFS spectrum of the $IF_6[Ag(SbF_6)_3]$ sample, calculated in the k range of 4.0–12.5 $Å^{-1}$. Experiment – (solid line); EXAFS model – (dashed line).

Very good agreement between the model and the experimental spectrum is found in a *k*-range from 4 $Å^{-1}$ to 12.5 $Å^{-1}$ and in the R range from 1.0 Å to 5.0 Å. Eighteen variable parameters were allowed to vary in the fit: two Ag–F distances and two Debye-Waller factors (σ^2), one for the two axial and the other for four equatorial F nearest-neighbors in the first coordination shell, seven neighbor distance and five Debye-Waller factors for the following seven coordination shells, and a common amplitude-reduction factor S_0^2 and the shift of energy origin E_o. The shell coordination numbers were kept fixed. A complete list of best fit parameters is given in Table 3. The quality of fit is shown in Figures 4 and 5.

4. Discussion

4.1. Synthesis

More than eighteen years ago oxidizing properties of solutions of Ag^{2+} in aHF were investigated.[18] It was found that when AgF_2 is dissolved aHF acidified with AsF_5, it oxidizes I^{5+} to I^{7+} (i.e. IF_5 was converted to IF_6AsF_6). After the isolation, the mixture of IF_6AsF_6 (~90 wt.%) contaminated with $AgFAsF_6$ was obtained.Three years ago part of this mixture was recrystalized in aHF yielding among powdered material colorless single crystals of IF_6AsF_6.[19] To prepare the IF_6SbF_6, the rest of the $IF_6AsF_6/AgFAsF_6$ mixture was treated with SbF_5 in aHF and recrystalized from aHF. Beside colorless crystalls of IF_6SbF_6, blue crystals had also grown. On the basis of their color it was expected that they correspond to $Ag(SbF_6)_2$,[6] however the routine check by X-ray diffraction analysis showed that the blue crystals belong to a completely new compound $IF_6[Ag(SbF_6)_3]$.[20] Synthesis of pure $IF_6[Ag(SbF_6)_3]$ was later done by reaction between IF_6SbF_6 and $Ag(SbF_6)_2$ in aHF according to Equation 1:

$$IF_6SbF_6 + Ag(SbF_6)_2 \xrightarrow[298\ K]{aHF} IF_6[Ag(SbF_6)_3]$$

$IF_6[Ag(SbF_6)_3]$ is a blue-sky colored solid. In contact with moisture it immediately decomposes and turns brown.

4.2. Crystal structure of $IF_6[Ag(SbF_6)_3]$

$IF_6[Ag(SbF_6)_3]$ crystallizes in the trigonal space group $P\bar{3}1c$ (No. 163). A consequence of this is that Ag atoms are located on *2d* special position (an intersection of 3- and 2-fold axis) and therefore they are found in a regular coordination of six fluorine atoms where all six Ag–F distances are equal to 2.189(7) Å. Such coordination is anomalous for ions with d^9 electron configuration (i.e. Cu^{2+}, Ag^{2+}) because they are strongly affected by the Jahn-Teller effect. Hexacoordinated Cu^{2+} compounds usually display tetragonal elongation along 4-fold axis with a coordination number (C.N.) 4+2 for Cu^{2+}. In the limiting case a square planar coordination may be found. Rare examples of a compressed geometry are also known.[21] For Cu^{2+} there are many examples where it had been initially reported on the basis of crystallographic data that some 6-fold coordinated Cu^{2+} compounds had regular octahedral coordination.[1,2] Further

investigations by other techniques (i.e. EPR, EXAFS) showed, that they have the usual Jahn-Teller tetragonally elongated octahedral configuration.[1,2] The reason of this phenomena are static Jahn-Teller (defined long axis is randomly distributed over three orientations relative to the unit cell axes) or dynamic Jahn-Teller effect (sufficient thermal motin to allow the long and short bonds in a structure to exchange over time).

Ag^{2+} has the same electronic configuratuion as Cu^{2+}. According to available literature data, in all known compounds, where Ag^{2+} is six-fold co-ordinated, AgL_6 (L = coordinated ligand) octahedra are elongated or compressed.[3] Since Ag^{2+} in $IF_6[Ag(SbF_6)_3]$ if is found in a regular octahedral coordination, EXAFS analysis has been done to confirm or disprove the results of X-ray structure determination of $IF_6[Ag(SbF_6)_3]$.

The EXAFS results clearly show that the first coordination shell is a distorted octahedron composed of six fluorine atoms: there are four short Ag–F bonds (2.11(1) Å) for the four equatorial F neighbors and two long Ag–F bonds (2.40(2) Å) for the two axial F. The Debye-Waller factors are found to be lower for the equatorial (0.008(2) $Å^2$) than for the axial F neighbors (0.012(3) $Å^2$). Similar distortion was found in the fourth coordination sphere composed of two F atoms at (3.84(5) Å) and four F neighbors at 4.14(7) Å. All other neighbor distances agree well with those obtained by XRD analysis.

As found by X-ray crystal structure determination of $IF_6[Ag(SbF_6)_3]$, the Sb–F bond lengths are equal to 1.839(7) Å and 1.848(7) for the terminal (F1, F2) and 1.933(7) Å for the bridging (F4) fluorine atoms of the $[SbF_6]^-$ anion. From Table 3 and Figure 1 it is evident that the individual distances between Ag and terminal fluorine atoms (F1, F1', F2) atoms obtained by two different methods are practically the same. Consequently, the values for Sb–F1 and Sb–F2 bond lengths obtained by X-ray crystal structure determination are realistic.

For Sb–F4 bond lengths this shouldn't be the case. Because if some of the Ag–F4 bonds are elongated and other compressed as found by EXAFS analysis, this should also influence on the corresponding Sb–F4 bonds. Additionally, X-ray and EXAFS distances between Ag and F4' (which bridges neighboring Ag' with Sb) should differ. For the later EXAFS gives two F4' atoms at (3.84(5) Å) and four F4' neighbors at 4.14(7) Å meanwhile X-ray data show there are six F4' atoms around Ag at equal distances (3.923

Å). That means that the value (6 x 1.933(7) Å) of Sb–F4 bond lengths obtained by X-ray is only an average. In reality there are two different sets of Sb–F4 distances (i.e. two shorter and four longer).

Table 3. Parameters of the nearest coordination shells around Ag atom in the $IF_6[Ag(SbF_6)_3]$ sample. For comparison, distances obtained by X-ray structure determination are also given.

	EXAFS analysis[a]			X-ray single crystal structure determination	
Ag neighbor	*N*	*R* (Å)	σ^2 (Å^2)	*N*	*R* (Å)
F4	4	2.11(1)	0.008(2)	6	2.189
F4	2	2.40(2)	0.012(3)		
F1	6	3.61(7)	0.02(1)	6	3.609
Sb	6	3.83(2)	0.011(2)	6	3.886
F4'	2	3.84(5)	0.004(2)	6	3.923
F4'	4	4.14(7)	0.004(2)		
F2	6	4.53(4)	0.005(3)	6	4.534
F1'	6	4.73(7)	0.005(3)	6	4.727
Ag'	2	4.79(7)	0.008(3)	2	4.778

[a]atomic species, average number *N*, distance *R* and Debye-Waller factor σ^2. A best fit is obtained with the amplitude reduction factor $S_0^2 = 0.97(8)$, E_o shift of 2 eV. Uncertainty of the last digit is given in parentheses.

$[IF_6]^+$ cations are located between infinite $[Ag(SbF_6)_3]^-$ chains. They are regular octahedra with all six I–F bond lengths equal to 1.778(7) and F–I–F angles between 89.2° to 90.9°. The I–F bond lengths and intra-ionic F···F distances (2.495 - 2.535 Å) are comparable to those found in $IF_6Sb_2F_{11}$ ($d_{average}$(I–F) = 1.779(6) Å, d(F···F) = 2.492–2.554 Å) [22] and IF_6AsF_6 (d(I–F) = 1.7744(17) Å, d(F···F) = 2.501–2.518 Å).[19] Because of the high symmetry each fluorine atom of the $[IF_6]^+$ cation is found in the same environment. Individual fluorine atom of the $[IF_6]^+$ cation forms one inter-ionic F···F contact (2.933 Å), with fluorine atom belonging to neighboring $[Ag(SbF_6)_3]^-$ chains, that lie within twice the van der Waals radius of fluorine (2.94 Å).[23] Second such contact is

already outside this value (2.985 Å). The shortest contacts (3.701 Å) between the fluorine atoms of the anions and the central iodine atom are outside the sum of fluorine (1.47 Å) and iodine (1.98 Å) van der Waals radii.[23]

3.4. Raman spectrum

Raman spectrum of $IF_6[Ag(SbF_6)_3]$ is shown in Figure 5 and frequencies and assignement are given in Table 4.

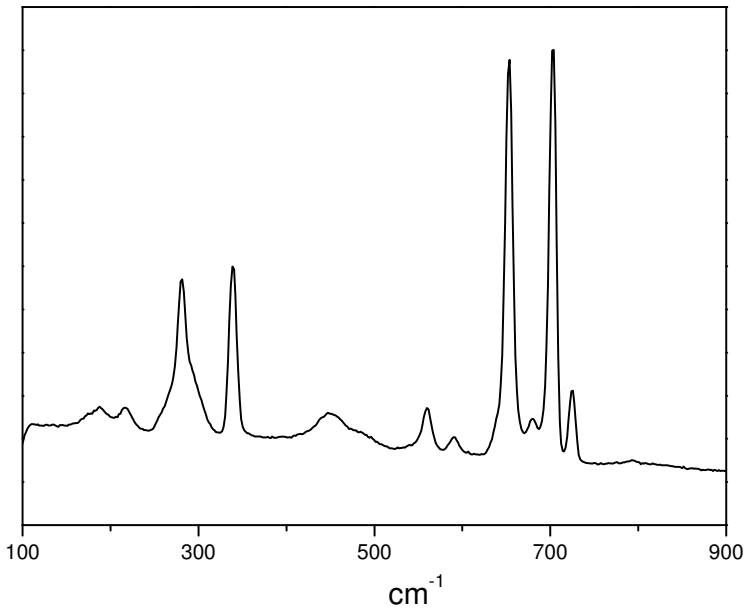

Figure 5: Raman spectrum of $IF_6[Ag(SbF_6)_3]$.

Table 4. Raman spectrum of $IF_6[Ag(SbF_6)_3]$.

Ra[a)]	assignments[b]
725(17)	$\nu_2'(IF_6)$
703(100)	$\nu_1'(IF_6)$
680(9)	$\nu_3(SbF_6)$
654(95)	$\nu_1(SbF_6)$
590(4)	
559(10)	$\nu_2(SbF_6)$
488(sh)	ν(Sb–F–Ag)
449(7)	ν(Sb–F–Ag)
338(42)	$\nu_5'(IF_6)$
294(sh)	$\nu_5(SbF_6)$
280(38)	$\nu_5(SbF_6)$

217(5)	$\nu_6'(IF_6)$	$\nu_6(SbF_6)$
190(5)	$\nu_6'(IF_6)$	$\nu_6(SbF_6)$

[a]Intensities are given in parenthesis; sh = shoulder.

The Raman spectrum exhibits bands which are characteristic for $[IF_6]^+$ and $[SbF_6]^-$, respectively. The strong Raman band at 654 cm^{-1} could be assigned to symmetric stretching (ν_1) mode and the weak ones at 559 cm^{-1} and 294/280 cm^{-1} to $\nu_2(SbF_6)$ and to bending (ν_5) mode, respectively. The weak bands at 488/449 cm^{-1} are in the region typical for Sb–F_b stretching modes.[24]

According to reported vibrational spectra of $IF_6Sb_2F_{11}$,[22] Raman bands at 725, 703 and 338 cm^{-1} could be readily assigned to stretching (ν_2' and ν_1') and bending modes (ν_5') of $[IF_6]^+$ cation. The ν_6' mode of $[IF_6]^+$ has never been observed. The calculation predicts that its frequency lie between 179 and 234 cm^{-1}.[] Since the ν_6 mode of $[SbF_6]^-$ is expected in the same region it can't be reliable to say if the bands at 190/217 cm^{-1} belong only to $[IF_6]^+$ or only to $[SbF_6]^-$.

The band at 680 cm^{-1} was observed also in Raman spectrum of IF_6SbF_6 [25] and it was assigned to a presence of impurity (i.e. $Sb_2F_{11}^-$ anion in of IF_6^+ salt). Since in the case of $IF_6[Ag(SbF_6)_3]$, the band at 680 cm^{-1} was also present in the Raman spectra recorded on single crystals, it has been rather tentatively assigned to the formally Raman inactive $\nu_3(SbF_6)$ mode because of the solid state effects. The origin of weak band at 590 cm^{-1} is not clear.

4. Conclusions

Ag K-edge EXAFS provides information on the local structure around Ag atoms in the sample. In this method the scattering of a photoelectron, emitted in the process of the X-ray photo-effect, is exploited to scan the immediate atomic neighborhood. Applying the EXAFS analysis to study the local environment around Ag in $IF_6[Ag(SbF_6)_2$, it was found that Ag has in usual Jahn-Teller distorted tetragonally elongated octahedral $[AgF_6]$ configuration (2 x 2.40(2) Å, 4 x 2.11(1) Å). This is in apparent contradiction with X-ray diffraction studies where $[AgF_6]$ octahedra appears to be regular octahedra (6 x 2.170(12) Å). The explanation of the apparently regular octahedral coordination of Ag(II) could be double. First is the tri-fold twinning (*drilling*)

of the monoclinic (as was observed in the case of ReO_3F [4]) or orthorhombic (β-AlF_3, [5]) unit cell, resulting in a pseudo trigonal/hexagonal lattice. Our attempts to find similar model were unsuccessful. Second reason could be static Jahn-Teller (defined long axis is randomly distributed over three orientations relative to the unit cell axes) or dynamic Jahn-Teller effect (sufficient thermal motion to allow the long and short bonds in a structure to exchange over time). If the disorder is dynamic, then the M–F bond lengths will be temperature dependet. In the case of static disorder and/or when the metal center lies on a special position the the M–F bond distances will be temperature-invariant and temperature ellipsoid analysis is necessary. However, even well-determined crystal structures do not show obviously enlarged temperature factors for the coordinated ligand atoms. Additionally, the fluxionality present at higher temperature (dynamic J.T.-effect) could be frozen out at low temperature (static J.T. effect). Such case reperesents $[Cu(LH)_2][BF_4]_2$ (L = organic ligand) where crystal structure has been determined in the 31 - 355 K temperature range.[1,2]

We haven't been able to find out which of the above mentioned reasons is valid in the case of $IF_6[Ag(SbF_6)_3]$. However, as shown also by this example, all reports about regular octahedral coordination, obtained from X-ray diffraction studies of metals with electronic configuration d^4 or d^9, should be taken with caution. As already proposed in an extensive reports of Cu^{2+} complexes,[1,2] these results should be checked by methods independet from crystal lattice.

Acknowledgement

This work has been supported by the Slovenian Research Agency research programme P1-0045, P1-0112 and P1-0021 by DESY and the European Community under Contract RII3-CT-2004-506008 (IA-SFS). Access to synchrotron radiation facilities of HASYLAB (beam-line C) is acknowledged. We would like to thank Edmund Welter of HASYLAB for expert advice on beam-line operation.

References

[1] M.A. Halcrow, *Dalton Trans*. **2003**, 4375–4384.

[2] I. Persson, P. Persson, M. Sandström, A.S. Ullström, *J. Chem. Soc. Dalton Trans.* **2002**, 1256–1265.

[3] W. Grochala, R. Hoffmann, *Angew. Chem. Int. Ed*. **2001**, *40*, 2742–2781.

[4] A. Le Bail, C. Jacoboni, M. Leblanc, R. De Pape, H. Duroy, J.L. Fourquet. *J. Solid State Chem.* **1988**, *77*, 96–101.

[5] J. Supeł, R. Marx, K. Seppelt. *Z. Anorg. Allg. Chem*. **2005**, *631*, 2979–2986.

[6] D. Gantar, I. Leban, B. Frlec, J.H. Holloway, *J. Chem. Soc. Dalton Trans*. **1987**, 2379–2383.

[7] Crystallographica Search-Match, version 2,1,1,0, Oxford Cryosystems, UK, 2003.

[8] TOPAS V2.1, Users Manual, Bruker AXS, Karlsruhe, Germany, 2000.

[9] SIR92: A. Altomare, M. Cascarano, M., C. Giacovazzo, A. Guagliardi, *J. Appl. Cryst*. **1993**, *26*, 343–350.

[10] Molecular Structure Corporation. (1997-1999). TeXsan for Windows. Single Crystal Structure Analysis Software. Version 1.0.6. MSC, 9009 New Trails Drive, The Woodlands, TX 77381, USA.

[11] G.M. Scheldrick, SHELXL-97, University of Göttingen, Germany, 1997.

[12] L.J. Farrugia, *J.Appl. Cryst*. **1999**, *32*, 837–838.

[13] DIAMOND v3.1. 2004-2005 Crystal Impact GbR, Bonn, Germany

[14] T. C. Ozawa; Sung J. Kang; "Balls & Sticks: Easy-to-Use Structure Visualization and Animation Creating Program", *J. Appl. Cryst.* **2004**, *37*, 679. http://www.softbug.com/toycrate/bs/

[15] A. J. Edwards and P. Taylor, J. Chem. Soc. Dalton Trans. 1975, 2174–2177.

[16] B. Ravel, M. Newville, J. Synchrotron Rad. 2005, 12, 537–541.

[17] J.J. Rehr, R.C. Albers, S.I. Zabinsky, Phys. Rev. Lett. 1992, 69, 3397–3400.

[18] B. Žemva, R. Hagiwara, W.J. Casteel, Jr., K. Lutar, A. Jesih, N. Bartlett, J. Am. Chem. Soc. 1990, 112, 4846–4849.

[19] E. Goreshnik, Z. Mazej, Acta Crystallogr. 2006, C62, i59–60.

[20] Z. Mazej, E. Goreshnik, 231st ACS national Meeting, Atlanta, 2006, Abstracts of papers.

[21] Z. Mazej, I. Arčon, P. Benkič, A. Kodre, A. Tressaud, Chem. Eur. J. 2004, 10, 5052–5058.

[22] J.F. Lehmann, G.J. Schrobilgen, K:O. Christe, A. Kornath, R.J. Suotamo, *Inorg. Chem.* **2004**, *43*, 6905–6921

[23] A. Bondi, J. Phys. Chem. 1964, 68, 441–451.

[24] LeBlond, N.; Dixon, D.A.; Schrobilgen, G.J. *Inorg. Chem*. **2000**, *39*, 2473–2487.

[25] F.A. Hohorst, L: Stein, E. Gebert, *Inorg. Chem*. 1975, 14, 2233–2236.